UNIVERSITATEA "POLITEHNICĂ" din BUCUREȘTI
FACULTATEA DE ȘTIINȚE APLICATE
Nr. Decizie _____ din _____

TEZĂ DE DOCTORAT

HIGH-PRECISION NUCLEAR SPECTROSCOPY IN NI ISOTOPES AND DATA ANALYSIS TECHNIQUE DEVELOPMENT

(SPECTROSCOPIE NUCLEARĂ DE MARE PRECIZIE A IZOTOPILOR DE NICHEL ȘI DEZVOLTARE DE METODE DE ANALIZĂ DE DATE)

Doctorand: Fiz. **Lucian STAN**

COMISIA DE DOCTORAT

Președinte	Prof. dr. Cristina STAN	de la	Univ. Politehnică București
Conducător de doctorat	Prof. Dr. Gheorghe CĂTA-DANIL	de la	Univ. Politehnică București
Referent	Prof. dr. Mihaela SIN	de la	Univ. București
Referent	CS I Dr. Nicolae Marius MARGINEAN	de la	INCD Fizică și Inginerie Nucleară „Horia Hulubei”
Referent	CS II Dr. Constantin MIHAI	de la	INCD Fizică și Inginerie Nucleară „Horia Hulubei”

BUCUREȘTI 2021

Chapter 1

Nuclear structure in the vicinity of shell closure

1.1 Evidence for the existence of nuclear shells

In chemistry and atomic physics, the noble gases have the lowest chemical reactivity out of all the elements. This particularity has lead to the understanding that electrons arrange themselves in shells when they are part of an atom, with the noble gases corresponding to the closure of these shells. This is one of the cornerstones of chemistry.

Going one step further, into the nuclear landscape, the evolution of the intrinsic structure of the nucleus with N and Z suggests a similar pattern of filling nuclear shells with certain numbers of protons or neutrons. One of the differences with respect to the atomic model is that there are two different shells, one for neutrons and one for protons, which, while interacting quite strongly, can still be viewed, to a point, as separate and independent.

For even-even nuclei, with few exceptions across the table of isotopes, the first excited state is a 2^+, originating from raising a pair of nucleons to a higher orbital. A feature of magic nuclei is that this first excited state is higher-lying compared to its neighbors. This is even more evident for doubly-magic nuclei, for which both the proton and the neutron numbers are magic.

Numerous other systematics indicate that a structural change takes place near the magic numbers, like the ratio of the energies of the first excited 4^+ and 2^+ states for even-even nuclei, which has a minimum near magic numbers and the transition strength between the first 2^+ and the ground state, $B(E2, 2^+ \rightarrow 0^+)$, which similarly exhibits minima at the magic numbers.

Thus, drawing a parallel with the atomic case and the electron shells, the nuclear structure experimental data and evolution point towards the fact that neutrons and protons also separately arrange themselves into shells that close when Z or N reach a magic number. This is the core tenet of the nuclear shell model.

However, such a correspondence is not easy to draw. The electrons in atoms 'orbit' (for lack of a better term) around the nucleus, the positive charge of which creates the

electric central potential that governs the atomic shells. This is not the case for the nuclei, for which the central potential is given by the previously closed shells and a description the nucleon-shell interaction is certainly non-trivial.

1.2 The Shell Model

The simplest form of the shell model is the independent particle model, which is only applicable close to magic numbers. In this representation, the valence nucleons move in a spherically-symmetric central potential generated by the core. The shell model orbits start to be filled from the bottom upwards in a sequential manner, separately for protons and for neutrons. The movement of the valence nucleons is seen as 'independent', meaning that they are not influenced by other valence nucleons or the nucleons in the closed shells except through the central potential.

The first test of the shell model was finding a spherical potential that allows the exact reproduction of the observed magic numbers. Such a potential was first proposed by Maria Goeppert Mayer and coll in 1949, and it can be written as follows:

$$V(r) = \frac{1}{2}\hbar\omega r + V_{l^2}\vec{l^2} + V_{ls}\vec{l}\vec{s} \tag{1.1}$$

The spin and parity of the ground state, as well as the magnetic dipole moment and electric quadrupole moment are given by the remaining valence nucleons and holes, as are those of the excited states that are created by exciting the valence nucleons to higher levels. In the obvious case when the number of either type of nucleons is very close to the next shell closure, but less, the system arranges itself as if the shell was closed, with imaginary particles called holes on the last level to be filled.

After the introduction of the strong spin-orbit coupling and with appropriately chosen parameters, the shell model was not only able to correctly reproduce the existing magic numbers, but also state spins, magnetic moments and other nuclear properties of a number of nuclei. This proved to be a major breakthrough in nuclear physics understanding and it paved the way for further development.

However, the potential in Eq.1.1 has given way to other mean field approaches that better reproduce certain nuclear properties over a wider range of nuclei. These start from an effective interaction, basically a bi-nucleon force that is parametrized depending on the properties that have to be predicted and the nuclei that are investigated. Then, this effective interaction is used to derive a mean-field potential that can then be used in shell model calculations.

The independent particle model presented above was an extraordinary success for nuclear structure physics and still holds an important didactic purpose, but its power

of prediction covers a large, but limited palette of properties of a limited number of nuclei.

However, simple considerations can still be helpful in determining the spins and parities of grounds states and excited states of nuclei close to shell closures, such as the fact that it more favorable from an energetic point of view for pairs of nucleons to couple their total orbital momenta to $j = 0$.

It must be noted that, far from the stability valley, for exotic nuclei, other aspects of the complicated nuclear force, such as the tensor part, can lead to the erosion of the known magic numbers, to their disappearance and the formation of new ones around new shell gaps. This is known as "shell evolution".

1.3 The Shell Closure at Z=28

The 28 magic number is a direct consequence of the strong spin orbit coupling. This coupling removes the degeneracy, leading to the spliting of the $1f$ shell into two parts, of which $1f_{7/2}$, which has l and s parallel aligned and thus a stronger attractive potential, is significantly lowered over the large gap between the $1d - 2s$ and $1f - 2p$ shell pairs. Since the $1f_{7/2}$ level can hold up to $2j + 1 = 8$ nucleons on top of the previous closed shell at 20, this creates the 28 magic number.

The element with 28 protons is called nickel, which is a transitional metal. Nickel has 5 stable isotopes. The current known isotope list is bracketed by the radioactive doubly magic ^{48}Ni and ^{78}Ni, spanning 32 nuclides. Even-even Ni isotopes between $N = 28$ and $N = 40$ have relatively low-lying excited 0^+ states, with energies ranging between 1.5 and 5 MeV. Each isotope in this region has at least two such identified states, with some having three.

1.4 Modeling the Ni nuclei

The Ni isotopes have been attractive targets for nuclear structure modelling and theoretical investigations since the early days of the shell model. Having a magic number of protons and with three doubly magic isotopes and one magic-semi-magic isotope, the Ni isotopic chain has been important not only to the development and verification of the Shell Model and its countless improvements, but also for the observation and study of phenomena such as shape coexistance and shell evolution.

For example, just looking at shape isomerism and the search for its appearance in medium-weight nuclei, numerous attempts were made over the years. One of the most

important development is the Monte Carlo Shell Model through the Quantum Monte Carlo Diagonalization method. This is used to solve quantum-many-body systems with two-body interactions. As opposed to the regular shell model calculations, where the Hamiltonian matrix elements have to be calculated for all possible pairs of Slater determinants in the Hilbert space, the QMCD method relies on choosing appropriate many-body basis vectors for the calculation of the eigenvalues.

The first states are determined through other methods. A new basis vector is then created using a certain value of the variable, σ_1. The Hamiltonian is diagonalized in the space created by the previous existing basis vectors and the new vector. The energy eigenvalue obtained with the new vector and without are then compared. If the new basis vector sufficiently lowers the energy eigenvalue, then it is added to the set of basis vectors. This process is repeated until enough basis vectors are available to obtain reasonable eigenvalues. However, because the procedure selects only the most important basis vectors, the diagonalization of the Hamiltionian in the subspace defined by these vectors is far more computationally tractable because it minimizes the subspace size by eliminating the less important components

However, even though the addition of new basis vectors improves the value of the energy eigenvalue, it never truly reaches perfect precision unless the number of basis vectors is sufficiently high. In order to account for this, an extrapolation has to be used. This is done by fitting the energy-energy variance function for sufficiently large numbers of basis vectors.

The great advantages of the Monte Carlo Shell Model are that it can treat a wide variety of states in the same model space and with the same Hamiltonian and the fact it can do tractable calculations with relatively large numbers of valence nucleons.

The Ni isotopes of interest in this thesis require the simulation of the full *pf* shell, sometime also including the $g_{9/2}$ and $d_{5/2}$ orbits. The MCSM can not only predict the binding energies, excited level energies, spins and parities, reduced transition probabilities, but also the deformations of the states and their make-up. This is done by diagonalizing the quadrupole matrix of each basis vector for the investigated state, giving the Q_0 and Q_2 quadrupole moments.

1.5 Particle-phonon coupling

Further away from the magic numbers, the addition of both valence neutrons and protons leads to large residual interactions, and the single particle orbits given by the spherical shell model are no longer in accordance with the experimental data. For such nuclear systems, new approaches were required in order to make predictions in an easier and more physically-transparent manner, such as the collective models that

focus on "group behavior" of the nucleons.

It is not trivial to treat such vibrations and rotations of a nucleus from a microscopic point of view. However, the addition of certain concepts can simplify the understanding and use of these collective treatments, such as the phonon. Phonons are virtual particles which can be used to simplify calculations. These behave as bosons, having integer spin values. Multiple bosons, identical or not, can exist at the same time, and their total angular momentum can be calculated using the m-scheme. Furthermore, the destruction of a phonon is also accompanied by the emission of a γ-ray, just as is the case for single particles changing orbits.

For doubly magic isotopes, it is difficult to excite nucleons to higher orbits, as is demonstrated by the high excited energies of the 2^+ levels in such nuclei. Furthermore, because all doubly magic nuclei are spherical and not deformed, there can be no rotational excitations. However, coherent vibrations of the nucleons may offer a far less energetically demanding way of exciting such nuclei. For nuclei that are close to doubly magic isotopes, single particle excitations can be coupled to these collective vibrations, creating a particle-phonon coupling. This creates a number of states called a multiplet based on the angular momenta algebra of the phonon and particle coupling. The identification and study of such states is complicated, as both the excitations of the core and the structure of the investigated nucleus must be well known.

1.6 Shape isomerism

In nuclear physics, isomers are excited nuclear states that have lifetimes that span a broad range from nanoseconds to years and longer. The long (compared to the nuclear scale) lifetime of nuclear isomers is due to the hindrance of the deexcitation or decay of the excited nuclear state by certain phenomena.

Shape isomerism is another kind of mechanism that can lead to the creation of nuclear isomers. For certain nuclei, the potential energy exhibits a secondary minimum for a certain deformation. This then hinders the γ-deexcitation to the ground state, leading to long-lived isomers.

However, shape isomerism-like phenomena were recently discovered in a far lighter mass-region. ^{66}Ni, a proton-magic nucleus, has four identified 0^+ states. Of these, the reduced transition probabilities from the third (prolate) level to the first excited 2^+ was found to be quite small, indicating significant retardation. The hindrance of the transition from the third excited state can be explained by a sizable potential barrier between this prolate state and the spherical ground state.

Chapter 2

γ-spectroscopy in neutron transfer reactions below the Coulomb barrier

2.1 Neutron transfer reactions

Neutron transfer reactions consist of the exchange of neutrons between the projectile and the target nuclei. The neutrons may be transferred from the projectile to the target nucleus (stripping) or the viceversa (pick-up). Neutron stripping reactions allow the examination of neutron-rich nuclei close to the valley of stability.

About five years ago, the nuclear structure group from IFIN-HH initiated an experimental program consisting in spectroscopy studies performed using neutron-rich loosely-bound beams at energies below the Coulomb barrier. The ^{62}Ni(^{13}C,^{12}C)^{63}Ni experiment was the first out of a series of transfer experiments performed at the 9 MV Tandem accelerator using the RoSphere spectrometer in its mixed configuration.

Neutron transfer reactions belong to the direct and intermediate categories of nuclear reactions. Single step reactions are characterized by a small number of nucleon interactions on the surface of the nuclei involved, and not in their volume. The reactions are also significantly faster than their compound nucleus counterparts.

Neutron transfer reactions tend to be favored by reaction Q-values that are close to zero. If there is extra available energy, such reactions will favor the population of excited states up to a level where most of the extra available energy is used up. For γ-spectroscopy experiments, this offers an incentive to increase the energy of the beam, which is counterbalanced by the opening of the fusion channel over the Coulomb barrier. The logical conclusion is the use of beam energies slightly below the Coulomb barrier.

In the case of a transfer reaction, in the laboratory reference system, the heavy target nucleus is considered static and the light projectile moves with a kinetic energy of several tens of MeV.

Some aspects of such a reaction are worthy of note. Unlike the fusion-evaporation case, the residual nuclei do not emerge with a single well-defined kinetic energy, but with a range of kinetic energies that depends on the details of the kinematics of the

reaction. Similarly, the direction of the velocity is also not uniquely determined, but forms a cone centered on the beam direction.

2.2 Dominant Direct Population Dependency on Q-value

The number of transfer reactions that can be envisioned is as high as the imagination of the experimenter will carry it. However, not all such processes are possible and even those that are allowed by the conservation rules that govern the nuclear realm may have significantly low yields that render them unusable in practice.

One of the most often cited requirements for high reaction yields is that the classical distances of closest approach between the two nuclei be similar in the initial and final cases. These are closely related to the Coulomb radial wave functions which are part of the integral that gives the DWBA amplitude, which is itself proportional to the reaction cross-section. If the two distances of closest approach are close in value, then the two Coulomb radial wave functions will overlap and the DWBA amplitude integral will have a large value.

For neutron-transfer reactions, lower Q-values are favored over larger ones, despite there being less energy available to overcome the Coulomb barrier. For nuclear spectroscopy experiments, the population of excited states in the residual nucleus is of interest. Of course, in order to populate such excited states, the system must have enough available energy, consisting of the sum of the Q-value and a fraction of the incident kinetic energy. Any states lying above this value will be inaccessible through the given reaction.

The population of the excited states, in accordance with the selection rules, is further limited by conditions placed by the total transferred angular momentum. Transfer reactions that involve low relative velocities of the target and projectile, such as sub-Coulomb barrier ones, tend to maximize the angular momentum transfer.

Neutron transfer reactions selectively populate nuclear states that can be viewed as a coupling between the core and the transferred neutron, hole or cluster on a certain orbit. Neutron and proton transfer reactions that lead to the same residual nucleus will also usually lead to the population of different levels.

2.3 Doppler Shift Attenuation Method

In the case of electromagnetic radiation, the Doppler effect manifests itself as a shift in the wavelength (and thus energy) of the observed quanta when the source has a radial velocity relative to the observer.

This phenomena can also be used to obtain nuclear level lifetimes of the order of $10^{-14} - 10^{-11}$ seconds in nuclear reaction experiments.

The conservation of energy in a nuclear reaction with an accelerated beam states that the residual nucleus will have a significant recoil energy. If the nucleus is produced in an excited state, the velocity might be large enough to observe a Doppler shift of the energy of the γ photon.

In order to best observe the Doppler shift in nuclear reactions, it is desirable to have a larger recoil energy (and thus higher beam energy), an observation angle that is as close to 0° or 180° as possible, good resolution detectors and large energy γ rays.

There are two main methods by which the Doppler shift can be used to determine the lifetimes of nuclear states in nuclear reaction experiments, the Doppler Shift Attenuation Method and the Recoil Distance Method.

The Doppler Shift Attenuation Method (DSAM) is used to determine nuclear lifetimes of the order of $10^{-14} - 10^{-11}$ seconds. Such lifetimes are comparable to the stopping time of the recoiling nucleus in the target in some reactions. This means that at least a fraction of the γ-rays will be emitted before the nucleus has been stopped by its interaction with the rest of the target, and these will be Doppler-shifted.

As such, the shifted energy will become

$$E_{sh}(t) = E_0 \left\{ 1 + \frac{v(t)}{c} * \cos(\theta(t)) \right\} \tag{2.1}$$

where $E_{sh}(t)$, $v(t)$ and $\theta(t)$ all depend on the time from reaction. There are two methods of extracting nuclear lifetimes from DSAM data. The first one uses the average detected γ-ray energy at a certain angle to extract the attenuation factor. The second method of extracting nuclear lifetimes using DSAM is by using lineshape fitting.

DSAM analysis in neutron transfer reactions is slightly complicated by the kinematics problem. Because the final state of such a reaction involves two nuclei, the residual nucleus and the ejectile, the momentum of the residual is no longer as well defined as in fusion reactions.

2.4 Recoil Distance Methods

The Recoil Distance Method uses a thin target and a stopper placed at a certain distance behind the target. Due to the thinness of the target, following the nuclear reaction, the residual nucleus is expelled from the target, traveling towards the stopper.

After the residual exits the target, it will move towards the stopper until it strikes the stopper that is placed at a set distance behind the target. The ratio between the stopper-target distance and the residual velocity will give the time of flight. If the residual is in an excited state after the reaction, it can deexcite either in-flight, between the target and the stopper, or at rest, after it reached the stopper. If emitted in-flight, the γ-ray's energy will be measured with a Doppler-shift. If emitted at rest, there will be no Doppler shift.

Taking into account the velocity of the nucleus and the target-stopper distance, the lifetime can be extracted from the ratio of Doppler-shifted γ-rays to the number of unshifted γ rays coming from the same transition. This ratio is usually measured for several target-stopper distances.

The above case applies to levels that have only direct feeding. However, if both direct and side feeding are present, the image becomes slightly more complicated. Thus, for an excited level where all the above levels are direct fed, the number of γ-rays emitted after hitting the stopper is

$$N_{stopped} = N(t) + \sum_i b_i N_i(t) \tag{2.2}$$

where $N_{stopped}$ is the number of γ emitted at rest from the level of interest, $N(t)$ is the number of nuclei still in the excited state of interest upon reaching the stopper, $N_i(t)$ is the number of nuclei that have remained in excited states that feed into the level of interest and b_i is the branching from the higher excited states to the level of interest.

Knowing the lifetimes of the above levels, the branching ratios and the direct feeding intensity ratios, the lifetime of the level of interest can be calculated by fitting the data with the above function. Great care must be taken in propagating errors, especially since the determined lifetimes are usually not independent (if τ_i was determined using τ_j).

2.5 Alignment and Angular Correlations

Determining the spins and parities of the excited states obtained in nuclear reactions is an important part of the work being done with the RoSphere array at IFIN-HH. These important physical characteristics can be obtained from the lifetimes of the states or

from comparisons with appropriate theoretical models.

However, these indirect methods do not always give accurate or unique results, which can lead to ambiguities or mistakes in assigning the spins and parities in the final level schemes.

The presence of multiple detectors at varying polar and azimuthal angles with respect to the beam axis does offer significant opportunities for angular correlations.

In nuclear reactions of the type used at the 9 MV Tandem accelerator at IFIN-HH, an accelerated unpolarized beam of ions impacts a similarly unpolarized target. However, the direction of the beam defines a polarization axis for the resulting nuclei, which are left in an axially symmetric state.

A γ-ray emitted from such a state would have an angular distribution that can be written as

$$W(\theta) = \sum_{\lambda\, even} B_\lambda(I) A_\lambda(\gamma) Q_\lambda(\gamma) P_\lambda(\cos\theta) \tag{2.3}$$

where $B_\lambda(I)$ are the alignment parameters, $A_\lambda(\gamma)$ are the angular distribution coefficients, $Q_\lambda(\gamma)$ are the solid angle correction factors and $P_\lambda(\cos\theta)$ are the Legendre polynomials. However, when experimental measurements are done, the first three terms are bundled together into coefficients for the Legendre polynomials which can be extracted from the measured distributions. Furthermore, only the dipole and quadrupole terms are usually taken into account, as the higher-order terms are neglected, usually being very small

$$W(\theta) = a_0 + a_2 P_2(\cos\theta) + a_4 P_4(\cos\theta) \tag{2.4}$$

However, information can be gathered by the detection of two γ-rays which are successive in a cascade, along with the detection of their relative direction. This is the $\gamma - \gamma$ angular correlations method. If the initial state has some sort of orientation (such as axial symmetry), then the method is called Directional Correlations from Oriented states (DCO).

However, for experimental set-ups such as RoSphere, the polar and azimuthal angles of the detectors are not at the researcher's choice. Such multi-detector set-ups present other opportunities. The large number of detectors leads to an impressive number of detector pairs that can register the γ-rays. Due to the axial symmetry of the set-up and the placement of the detectors, these detector pairs can then be arranged in groups based on their relative positions, for which $E_\gamma - E_\gamma$ matrices can be created. Each group corresponds to a certain $\theta_1, \theta_2, \varphi_2 - \varphi_1$ set of parameters. The obtained experimental values allow for a fitting of their directional correlation function and thus the spins of the states and mixing ratios of the transitions connecting them may be obtained.

Chapter 3

Event mixing software package for angular correlations in transfer reactions

---

^{63}Ni's medium nuclear weight and position inside the valley of stability have made it an attractive research and experiment subject for the last seven decades. The ^{63}Ni entry in the ENSDF database contains evaluated data from no fewer than 36 different articles spanning from 1956 to 2012. The XUNDL database contains yet-unevaluated data from another five articles spanning from 2011 to 2017.

In 2015, during a lull in the experimental campaign, a test was undertaken using the RoSphere experimental set-up and the 9MV Tandem accelerator. A beam of ^{13}C was accelerated and impinged on a ^{62}Ni target. The beam energy was chosen to be 28 MeV, slightly below the Coulomb barrier. ^{63}Ni was the reaction product the test aimed at studying, produced in the ^{62}Ni(^{13}C,^{12}C)^{63}Ni reaction. Due to some delays suffered by the experiment that should have followed, the ^{63}Ni test-experiment was maintained for 5-6 days. The test was a success, spawning tens of new proposals and experiments employing transfer reactions at the 9MV Tandem in the subsequent years.

Due to the longer-than-expected beam time and the large number of detectors in the RoSphere array, it was possible to measure the properties of a number of excited states in ^{63}Ni using fast-timing or DSAM measurements for lifetimes and angular correlations for the determination of spins and parities.

For the initial experiment, the RoSphere array was in the standard configuration of that period, mounting 14 Compton-shielded HPGe semiconductor detectors. The HPGe detectors were placed as follows: 5 detectors in the 37° ring, 5 detectors in the 143° ring, 3 detectors in the 90° ring and the final one in the 110° ring. The target used was a self-supported, 10 mg/cm^2 isotopic ^{62}Ni one.

Despite the abundance of experiments that have studied the nuclear structure of ^{63}Ni, its low-spin level scheme is not well known. Taking advantage of the excellent energy resolution of the HPGe detectors in the RoSphere array, coupled with the ability to record coincidence information from these detectors, we were able to significantly expand the known level scheme. 24 new transitions that were not identified until this

work were added and three transitions are just tentative. All the states involved in these transitions were already known from previous experiments, although their evaluated excitation energies often had large uncertainties, of the order of 10 keV. Our measurements allow the determination of these excitation energies with far better precision.

Using the coincidence information obtained from the γ-γ matrices along with intensity balances, the new γ-transitions were placed in the level scheme, as can be seen in Fig.3.1. The fact that the placement of the new transitions was compatible with the already available information on excited states in ^{63}Ni lends additional credence to our assignments.

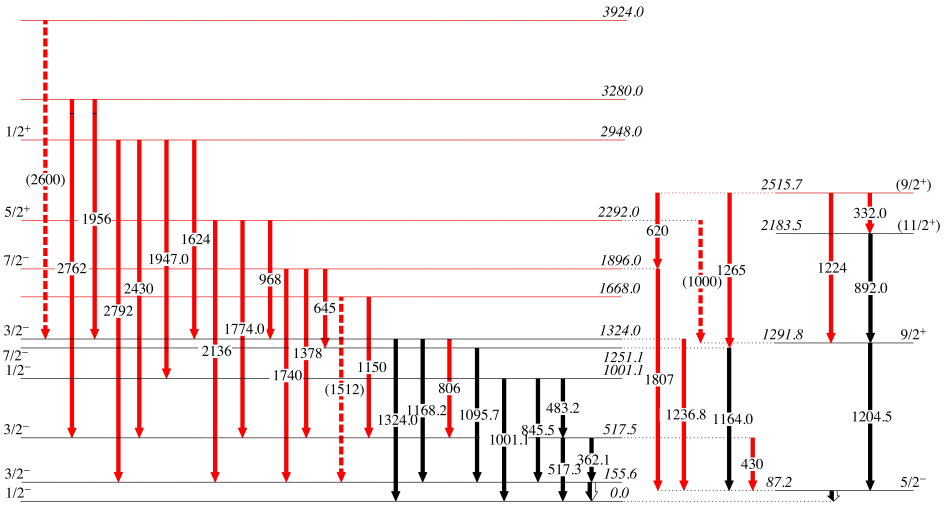

Figure 3.1: The level scheme of ^{63}Ni, as obtained from this experiment. 24 new transitions have been identified and placed in the level scheme and are represented with red. Three more transitions are just tentative due to very low statistics.

Efficiency-corrected peak intensities were also extracted from the data, allowing the calculation of branching and direct population ratios which were then used in the DSAM lifetime determinations.

Just a few of the known excited levels have measured lifetimes. Given the excellent

timing and energy resolution capabilities of the ROSPHERE array, we were able to extract lifetimes using the DSAM and fast-timing techniques. For the DSAM measurements, the measurements were carried out using two methods, lineshape fitting and centroid-shift.

The obtained lifetimes were used to extract the reduced transition probabilities and determine the character of the γ-transitions and, thus, either determine or restrict the spins and parities of the involved states.

The spins and parities of a number of the already known excited states in ^{63}Ni have already been determined in previous experiments, while for others only tentative assignments are available, and the experiment undertaken using the RoSphere array presented an excellent opportunity to verify and expand these assignments.

The large number of detectors and of available detector-detector angles meant that the current experimental data was especially suitable for angular correlations and DCO analysis. For this, the possible combinations of thirteen of the available HPGe detectors were split into eleven DCO groups based on the angle between the detectors and with respect to the projectile beam.

For each of the eleven defined groups, separate γ-γ matrices had to be sorted from the available runs. For normalization, the Jumbler program and the data mixing procedure for data normalization presented in Chap.5 were used. Two sets of eleven group matrices were prepared, each packaged into an index-$E_{\gamma_1} - E_{\gamma_1}$ cube. The first set, further named the data set, represented the splitting of the data into the eleven DCO groups, with the required time gates.

All possible pairs of γ-transitions from Fig.3.1 were investigated. However, only 32 such pairs could be analyzed, while others could not be investigated due to poor statistics.

For each pair of γ-transitions, peak and background gates, along with area factors, were input into the Bash program to extract the group intensities. Separate normalization gates usually had to be selected, using intense unshifted γ-transitions from the experimental spectrum. The script would then also extract the normalization values and apply them to the group intensities in order to extract the normalized intensities. Error propagation was also carried out.

After the normalized intensities for the eleven groups were obtained, these were fed into the Corleone program, along with the relevant angles for the groups. In order to fit them, hypotheses for the spins of the three involved levels had to be input. The program then output a number of possible solutions, each with a χ^2 value of the fit, the width of the spin distribution (σ) and the mixing ratios for the two transitions. If necessary, the spin distribution width or the mixing ratios could be set to a certain value.

For the 16 excited levels investigated, a number of spin hypotheses were selected and then tested by fitting with the Corleone program. The analysis was done from

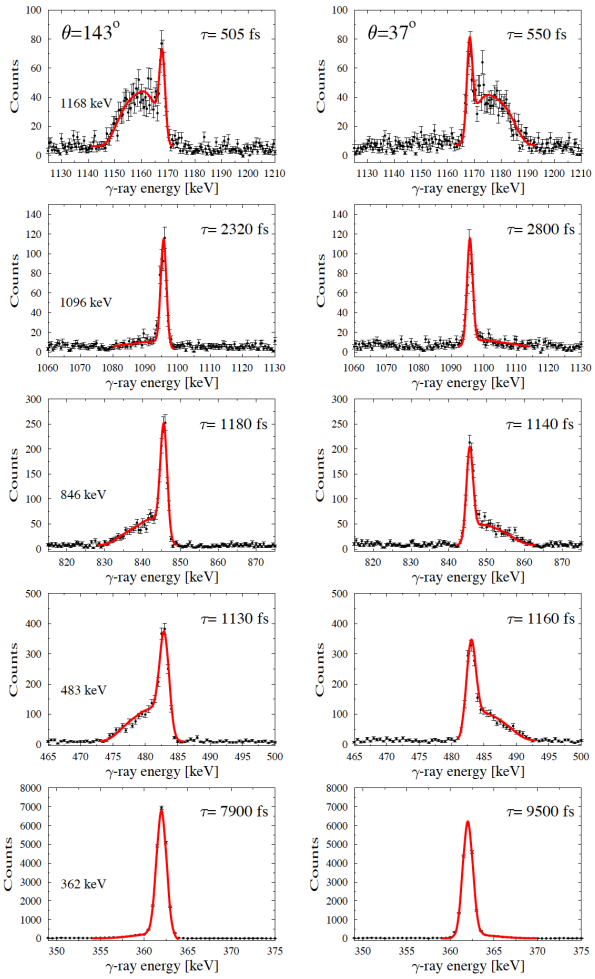

Figure 3.2: γ-ray lineshape DSAM fits from the low-J side of the ^{63}Ni level scheme. Spectra taking from the forward and backward detectors are on the right and on the left, respectively. The transition energies and the obtained lifetimes are marked on the each plot.

the bottom of the level scheme upwards. For each spin hypothesis combination, the possible solutions were recorded in a table for further cross-verification. The solutions were considered possible if they had physically-compatible values for the width of the spin distribution and the errors of the mixing ratios.

After all the solutions were gathered, these were cross-checked for compatibility. Cascades passing through the same level had to be compatible with the same spin assignment for that level. Similarly, the mixing ratios for each transition had to be compatible between different cascades containing that transition.

Following this procedure, definite spin assignments were obtained for 9 of the 16 levels in the ^{63}Ni scheme. 5 of these are in agreement with the literature assignments. For 3 of these excited levels, the spin was in agreement with the tentative value given in the literature. For one of these levels, there were no prior assignments in the literature.

Of the other 7 levels, for 5 of them, more than one spin assignment was compatible with the data. 3 of them were compatible with 2 different spin assignments, while for 2 of them, 4 spin assignments were in agreement with the data.

Of the 37 γ-transitions in the level schemes, mixing ratios could be assigned to 14 of them. In all of the 14 cases, the mixing ratio assignments were in agreement for all of the investigated cascades. For each γ-transition, the mixing ratio value is the result of a least square fit through all of the available mixing ratios from all the cascades in which it is present.

Unfortunately, for 11 of the transitions in the level scheme, the mixing ratio could not be determined because at least one of the spins of the excited levels involved was not uniquely identified. Depending on the spin assignment for these levels, the mixing ratio was different. However, since the spin could not be determined with the available data, neither could the mixing ratio.

For the other 12 transitions, insufficient statistics was available in order to perform a DCO analysis or the gates could not be cleared of contaminants.

3.1 Conclusion

This chapter has presented the adaptation of the Event Mixing software for DCO analysis using the RoSphere array and the GASPware and Corleone analysis suites. This software allows for the reliable normalizations on data obtained using RoSphere, increasing the reliability of the subsequent DCO analysis. DCO analysis was then performed for ^{63}Ni, yielding spins of excited levels and mixing ratios of the connecting transitions.

Chapter 4

Lifetime determinations for excited levels in ^{64}Ni using the plunger device in a sub-barrier two-neutron transfer reaction

Shape isomers are nuclear excited states that are hindered from deexciting by differences between their shape and the shape of the states they would deexcite to. Theoretical calculations have identified lighter shape-isomer candidates starting from 1989. Most of these studies identified Ni isotopes as the lightest nuclei that could exhibit such phenomena. Of these, the ^{66}Ni isotope was presented as a likely candidate in several studies, and was selected for further investigation through MCSM calculations and experimental investigations. The calculations predicted the existence of four 0^+ states in ^{66}Ni. The last 0^+ state, which is heavily prolate, is separated from the spherical ground state by a sizable saddle in the PES, indicating that its deexcitation to spherical states might be significantly hindered.

An experiment was undertaken at the 9MV Tandem accelerator in Bucharest to study these states. The experiment was undertaken using a thin target and the Bucharest Plunger device, allowing lifetime measurements to be taken using the RDDS method. The fourth state was identified and, following RDDS analysis, its lifetime was extracted ($19.6^{+(7.5)}_{-(6.6)}$ ps) 0^+. The corresponding B(E2) values for this transitions is 0.21(7) Weisskopf units, showing significant hindrance.

The retardation of the fourth (prolate) 0^+ state was explained by the significant potential barrier between this state and the spherical ground state minimum. This made ^{66}Ni the lightest nucleus in which shape-isomer-like structures have been identified up until this point.

Following the successful search for shape-isomerlike structures in ^{66}Ni, attention turned towards the ^{64}Ni isotope. The same Monte Carlo Shell Model calculations also predicted the appearance of the same phenomena in ^{64}Ni, as can be seen in Fig.4.1.

Only two 0^+ excited states had previously been identified in ^{64}Ni. Also, only a single one of these excited states had a measured lifetime of 0.04(2) ps, with a very

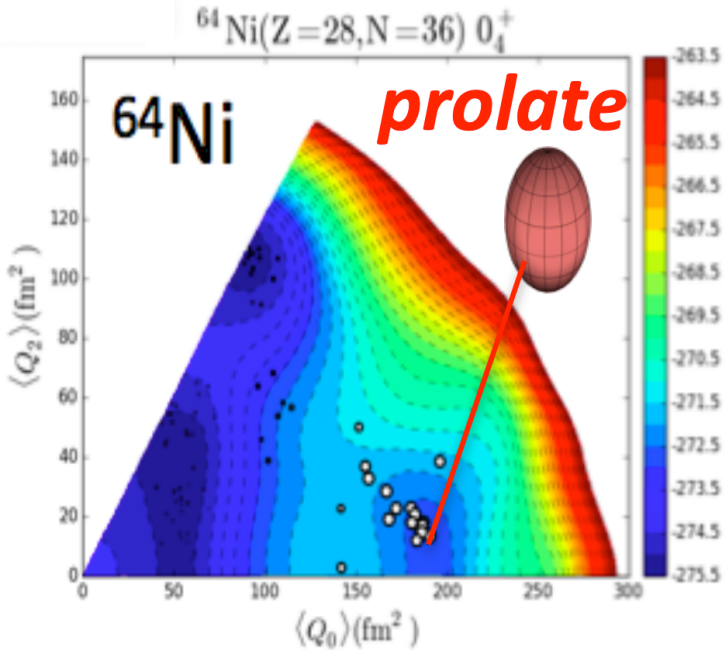

Figure 4.1: The potential energy surface of the 0^+ states in the ^{64}Ni isotope as calculated using Monte Carlo Shell Model Calculations. Four 0^+ states appear again, two spherical, one oblate and one prolate, as in ^{66}Ni. The prolate one, shown in this figure, is separated from the spherical ground state minimum by a potential barrier that should lead to a longer-than-expected lifetime.

large uncertainty.

In order to investigate these aspects and gather more spectroscopic information about the excited levels and nuclear structure of ^{64}Ni, an experiment was proposed at the 9MV Tandem accelerator in IFIN-HH. The experiment was split into two parts, the first an angular distribution measurement. The purpose of this section of the experiment was to investigate the angular distribution of 2503 keV transition from the 3849 keV state in order to ascertain if it is a 0^+. The 2124 keV γ-transition from ^{11}B, populated in inelastic scatterings, overlapped over the 2503 keV γ-ray of interest at certain angles due to a significant Doppler-shift. Despite this and somewhat poor statistics, the experiment lead to the conclusion that the 3849 keV level investigated was not a 0^+.

The second part of this ^{64}Ni experiment consisted of an RDDS measurement using the RoSphere array and the Bucharest plunger device. ^{64}Ni was produced in the ^{62}Ni(^{18}O,^{16}O)^{64}Ni two-neutron transfer reaction, with the ^{18}O beam having an energy slightly below the Coulomb barrier in order to suppress any competing fusion reactions.

Six different target-stopper distances were used in this experiment. The recoiling residual ^{64}Ni nuclei exited from the thin target with a velocity of 6.43 $\mu m/ps$.

The data from the 15 HPGe detectors was analyzed in order to extract the lifetimes of excited levels in ^{64}Ni using the Recoil Distance Method. No new γ-rays or excited levels were observed compared to those already known.

Lifetimes were obtained for a number of the excited levels for which γ-transitions were observed. Because the only suitable gating condition was on the $2^+ \rightarrow 0_1^+$ 1345 keV γ-ray, only the unshifted peak was observed for each γ-transition in ^{64}Ni.

While the BGO-detectors used for anti-Compton shielding have very poor energy resolutions, they have very large dimensions and excellent γ-ray detection efficiency. This opened up the possibility of constructing a multiplicity filter for the data analysis.

For each of the six target-stopper distances used in this experiment, peak intensities were extracted for the γ-transitions of interest using a gate on the $2^+ \rightarrow 0_1^+$ 1345 keV γ-ray. The multiplicity filter was used for certain transitions, while others were analyzed without this feature.

For the two known 0^+ states in ^{64}Ni, which have no feeding in the reaction used in this experiment, the intensities were obtained from matrices with multiplicity two only, as it is expected that they would only appear in combination with the 1345 keV transition. The intensities as a function of the flight time were then fitted with a simple exponential.

This analysis for the first excited 0^+ state at 2867 keV can be seen in Fig.4.2, yielding a lifetime of 1.362±0.288 ps. A similar analysis for the second excited 0^+ state at 3026 keV gives a lifetime of 3.917±0.389 ps.

A special problem was posed by the 359-323-1239-1264 keV γ-cascade. Because these levels decay one into another, there is significant above-feeding which complicates the fitting procedure, requiring knowledge of the lifetimes, populations and branching ratios of above levels and more complicated Bateman formulas.

These Bateman equations are significantly more complicated than the simple exponential, especially through the appearance in the formulas of the lifetimes and feeding ratios from other levels. Even so, this is a simplified case in which each level is fed by only one other transition.

Fitting the experimental data and extracting the lifetimes of the levels of interest requires knowledge of the lifetimes of the preceding levels and of the feeding ratios, which can either be extracted from the data or from the same fit. It is certainly preferable to extract the values from other fits and then include them as parameters into the new fit, as this limits the free parameters and improves the quality and errors of the fitting procedure, but this is not always possible.

Less simple, however, is how to correctly and transparently propagate the errors that are associated with the other lifetimes and feeding ratios through the fit. This is crucial in order to be able to publish reliable data with correctly estimated errors.

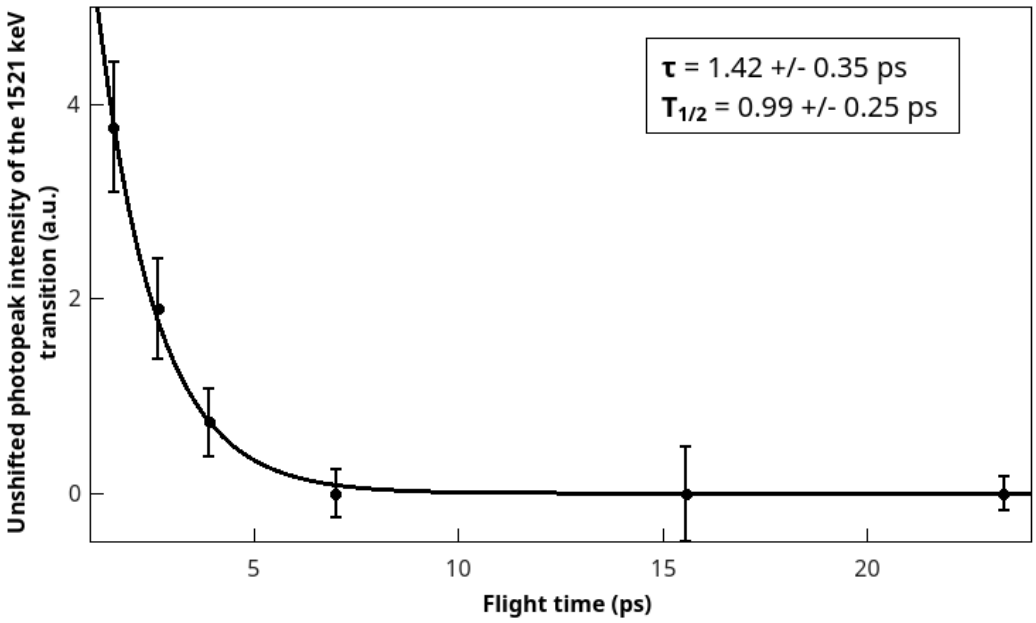

Figure 4.2: Determination of the lifetime of the first excited 0^+ state at 2867 keV using the RDM method. Data from only three distances could be used because the 1521 keV peak becomes unobservable at larger distances. The determined lifetime is of 1.362±0.288 ps.

In order to address this issue, I have devised a simple solution using a Monte Carlo fitting procedure employing the ROOT programming language. Due to the tremendous power of modern-day computers, millions of fits can be done in just a couple of minutes. This allowed to not only fit the data using the other previously extracted parameters, but to also vary these parameters within their errors. All of these values are then used to extract the total error of the fit which contains both the error of the fitting procedure and the propagation of the errors from the previous values used in the fit.

The data analysis proceeded from the top downward. The normalized intensities of the 359 keV γ-ray were fitted with a simple exponential. For the following 323 keV γ-transition,the following formula was used

$$N_1(t_f) = N_1(0) * e^{-\frac{t_f}{\tau_1}} + N_0(0) * \frac{\tau_1}{\tau_0 - \tau_1} * (e^{-\frac{t_f}{\tau_0}} - e^{-\frac{t_f}{\tau_1}}) + N_0(0) * e^{-\frac{t_f}{\tau_0}} \qquad (4.1)$$

where τ_0 is the lifetime of the 4531 keV level obtained previously using the 359 keV γ-transition and $N_1(0) = f_r * N_0(0)$, where f_r is the ratio of the number of nuclei populated directly in the 4172 keV excited state divided by the number of nuclei populated directly

in the 4531 keV excited state. For our case, f_r was determined to be 0.558 ± 0.106 from a previous test run with a thick target undertaken with the RoSphere array.

However, instead of using $\tau_0 = 12.514$ ps and $f_r = 0.558$ and simply fitting with these values, we have instead done a million fits with τ_0 and f_r distributed on a random Gaussian centered on these values and with $\sigma_\tau = 1.318$ ps and $\sigma_{f_r} = 0.106$, respectively. Each fit resulted in a τ_1 value and its associated error, which were then used to add 100 points, also distributed on a Gaussian, to a result histogram. After a million such fits, fitting this histogram with a Gaussian allows the extraction of the final τ_1 value and its associated error.

Similar analysis, albeit using even more complex formulas, was also performed for the subsequent 1239 and 1264 keV transitions.

Of the eleven excited states for which we have extracted half-lives, only two had been previously measured according to the ENSDF database.

For the 2610 keV level, the ENSDF file for ^{64}Ni gives a half-life of 1.73 ps, almost two times lower than the value extracted here of 3.37 ps. While the 2610 keV level does receive important cascade feeding, this accounts for only 10% of the observed intensity, the rest coming from direct population.

The 2610 keV level was measured and was given a lifetime of 1.73(28) ps from analysis of the lineshape from the spectrum obtained from the single 24%-efficiency HPGe detector placed at 0°.

The half-life of the 2867 keV 0_2^+ level was given to be 40(20) fs, in clear contradiction with the 937(199) fs extracted in this work. The value of 40 fs for the half-life is incompatible with the observed recoil distance decay curve.

The most important results from this analysis are the lifetimes for the two known 0^+ excited levels at 2867.3 and 3025.9 keV. The obtained half-lives are 0.93(20) and 2.71(27) ps, with the corresponding B(E2) reduced transition probabilities of 4.8(10) and 1.02(10) W.u. Neither of these values indicate any hindrance, as was sought after in this experiment, but such a hindrance is expected for the third excited 0^+ state which could not be identified in the experiments using the RoSphere array.

4.1 Conclusion

This chapter has presented the analysis of the lifetimes of excited nuclear states from ^{64}Ni extracted using the RDM method following a neutron-transfer reaction. The RoSphere array and the Bucharest plunger device were used for these measurements.

Despite the fact that the sought-after third excited 0^+ was not identified, the extracted lifetimes will prove useful for understanding the nuclear structure of ^{64}Ni. The lifetimes of the other two excited 0^+ states do not have any hindrance.

Finally, a procedure was developed for propagating errors across multiple lifetime fits using Root routines.

Chapter 5

Software package for normalization in angular correlation measurements. Angular correlations in ^{64}Ni using the FIPPS array

---

In order to better investigate the excited nuclear states in ^{64}Ni, an experiment was proposed at the Institute Laue-Langevin in Grenoble, France, using the FIPPS array consisting of 16 Compton-shielded HPGe detectors. Bearing designation 3-17-36, the experiment took place in 2019 over a period of 20 days.

The experiment was performed using a radioactive target containing nickel oxyde placed in a flux of thermal neutrons from the ILL reactor. The nickel content of the target was made up of roughly 10% ^{63}Ni, with the rest composed of ^{62}Ni and traces of other Ni isotopes. Through neutron-capture on ^{63}Ni, the 9657 keV 1^- capture state in ^{64}Ni was populated, thereafter decaying through various other low-spin levels. Because the radioactive target also contained significant quantities of ^{62}Ni, ^{63}Ni was also produced during this experiment and could be similarly investigated.

The large efficiency of the FIPPS array, coupled with the high-resolution of the HPGe detectors and their large numbers make them perfect for the construction of excited level schemes using the detected γ-transitions, the coincidence relationships between them and their relative intensities. Furthermore, due to the large number of detectors and the large number of detector pairs opening angles, data obtained using the FIPPS array lends itself very well to angular correlation analysis. Because the neutron capture-reaction leads to a completely isotropic spin-distribution, there are no alignment corrections that need to be accounted for during the analysis.

In order to obtain the angular correlations, a correction for the differing efficiencies of the crystals due to their placement and construction is required. Finding a solution to the problem of the normalization of the data for angular correlation and DCO measurements is paramount. Otherwise, certain values cannot be extracted at all or will have very large associated errors, limiting the amount and usefulness of the obtained nuclear structure information.

An attractive alternative to efficiency fitting or normalizing using certain γ-ray pairs was presented by the GRIFFIN team at TRIUMF. Their method of event-mixing has the advantage of being applicable to any γ-ray pair, regardless of their energy, and of also using the data itself for the normalization, with all the associated variations in the parameters of the detectors and DAQ built in.

In order to obtain this normalization, the γ-ray pair that is to be studied is used for the normalization following an event-mixing procedure. In this procedure, the real coincidence events recorded by the DAQ system during the experiment are broken up and the information from each detector is randomly paired-up into 'fake events' with detector signals from another time-uncorrelated event.

Ideally, this procedure creates a γ-γ-angle intensity matrix that maintains the same efficiency and coincidence terms as the original data, but replaces the physical angular correlation between the two transitions with an isotropic distribution. The γ-γ-angle intensity matrix can then be used to produce normalization values for any transition pair at any angle and then be used to divide the real data in order to obtain a corrected angular correlation plot that can be fitted.

In order to implement this procedure, a combination between the gsort routine from the GASPware package and a special program that was written using C++ and Qt libraries was used.

In order to validate the functioning of the procedure, a series of tests were conducted in order to verify the functioning of the programs and the best possible parameters for it. Verifications were done using the well-know $0^+ \rightarrow 2^+ \rightarrow 0^+$ 1680-1345 keV cascade. The angular correlations for this cascade, as explained previously, should have no mixing ratio effects and depend only on the known spins, leading to a unique solution to the fitting.

The theoretical values for the A_2 and A_4 coefficients for a $0^+ \rightarrow 2^+ \rightarrow 0^+$ cascade are $A_2 = 0.357$ and $A_4 = 1.143$. The benchmark normalization yields $A_2 = 0.346 \pm 0.003$ and $A_4 = 1.080 \pm 0.003$, as can be seen in Fig.5.1.

By far the most dramatic proof of the value of this normalization procedure was given by the 483-362 keV $1/2^- \rightarrow 3/2^- \rightarrow 3/2^-$ cascade from ^{63}Ni. The angular correlation using the usual normalization was already shown in Fig.5.2, presenting a very large scatter of the points. This is caused by the fact that the normalization used was based on a pair of transitions in which one of the γ-rays was of very high energy, and thus the efficiency ratios of the detectors were not the same as for the low energy 483 and 362 keV transitions.

The angular correlations obtained using the new normalization are show in Fig.5.2 and show a dramatic improvement both in the error of each individual data point and in their scatter. This new normalization allows us to confidently extract the A_2 and A_4 values for this cascade, although the mixing ratios cannot be trivially obtained because both transitions can have non-zero mixing ratios, leading to a non-unique so-

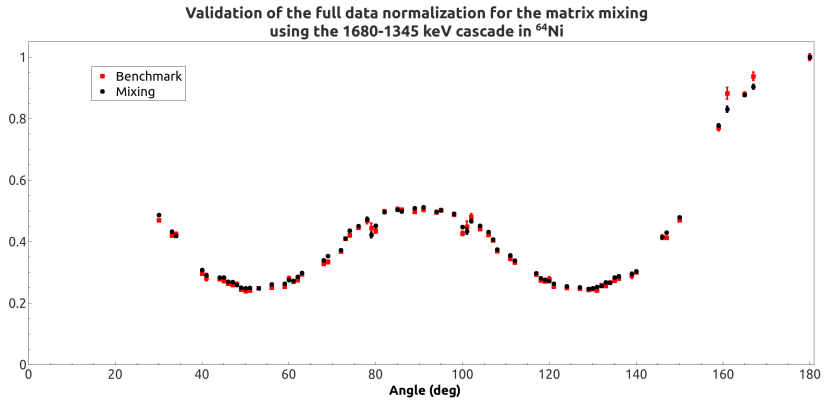

Figure 5.1: A comparison between the final normalization obtained from the mixing procedure and the benchmark normalization used on the 1680-1345 keV γ-cascade. The red squares show the benchmark obtained using the 6630-1680 keV $1^+ \rightarrow 0^+ \rightarrow 2^+$ cascade from ^{64}Ni. The black dots show the data normalized using a multiplication factor of 10 and the entire data set.

lution. Nonetheless, this plot clearly emphasizes the utility of this new procedure for normalization, which will hopefully shortly lead to its widespread adoption for RoSphere and FIPPS experiments.

Following these results, it was decided to analyse the rest of the ^{64}Ni data from the FIPPS experiment using this procedure.

For the angular correlation analysis to be performed, two γ-γ-angle intensity matrices are required, the data matrix and the mixed matrix. They both contain the exact same run-by-run calibrations, time gates on HPGe and BGO signals, and the same addback procedure. The main difference resides after these operations have been completed. While the data matrix is constructed immediately after these procedures, for the mixing matrix, the data is then written to disk in a reduced 'cut' format.

The 'cut' data files are then fed into the Jumbler program. This program destroys the true events and produces 'Mixed' files in which the signals have been randomly paired to form 'fake' events. These 'Mixed' files are then sorted into a $\gamma - \gamma$-angle intensity matrix as has been done for the data matrix.

For the first chosen γ in the cascade, three γ-angle intensity matrices, corresponding to the γ-peak and the other two corresponding to the background, are extracted. The background matrices are then substracted from the peak matrix using a multiplication factor, yielding an intermediary background-substracted matrix.

This *gamma*-angle intensity matrix is then cut into three vectors, one corresponding to the second γ-peak and the other two corresponding to its background intervals, which are then again substracted to yield a final angle intensity vector. This results in

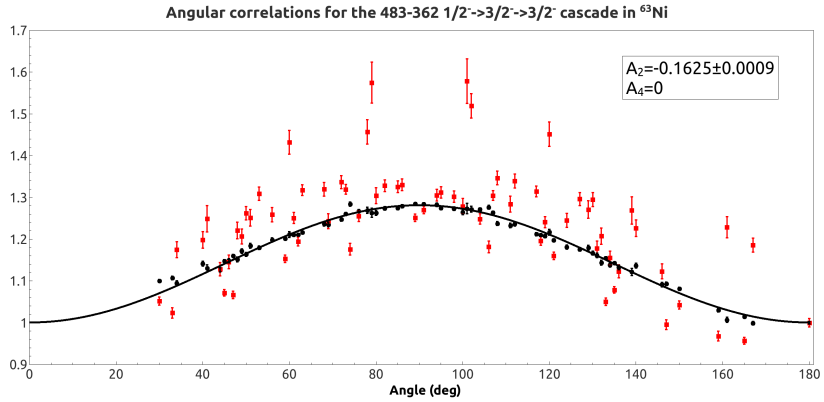

Figure 5.2: Angular correlations of the 483-362 keV $1/2^- \rightarrow 3/2^- \rightarrow 3/2^-$ cascade from ^{63}Ni using the normalization obtained with the current procedure (black dots) and another normalization obtained using two angularly-uncorrelated *gamma*-transitions.

two angular correlation vectors with the intensities as a function of the angle.

The ratio of the two vectors will be the angular correlation function for that particular γ-cascade, which can then be fitted to obtain the experimental A_2 and A_4 parameters. In our case, the fitting procedure was done with a simple ROOT program that returned the A_2 and A_4 values and their errors, which are then used to investigate the spins of the involved levels and the mixing ratios of the two transitions.

A number of γ-cascades from ^{64}Ni were analyzed using this method using data taken with the FIPPS array at ILL. For most of these analyzed γ-rays, I have tried to find cascades with other transitions with no mixing ratio, such as those involving a level with spin-parity 0^+. This allows a unique determination of the mixing ratio of the other transition. However, in cases where no such 0-mixing-ratio partner could be found, a transition that has its mixing ratio determined is preferable. This is the case of the 7380-930 cascade, where the 930 keV transition was studied using three other cascades, giving an average $\delta_{930} = 0.73$, which was then used in the fitting.

5.1 Conclusion

This final chapter has presented the implementation of the event-mixing normalization technique for GASPware-format data taken using the FIPPS array. However, this procedure can be easily implemented for any data taken in the GASPware format, such as with the RoSphere array.

The procedure has been benchmarked by comparing it with other normalization

procedures, yielding excellent results. This will be adopted for future measurements as well, as the use of angular correlations has offered valuable spectroscopic information. Furthermore, the use of this procedure for DCO analysis like that discussed in chapter 3 will be investigated.

Improvements to the procedure implemented will also be investigated and implemented in order to improve the reliability, precision, speed and disk usage of the program.